5 - Results and Discussion

5 - 1 DC-Conductivity:-

The temperature dependence of DC conductivity has been studied for all investigated samples over a temperature range between 300–773˚K.The result obtain are shown in Fig.(8).$\sigma_{d.c}$ was found to vary with composition of samples as stated in Table (5) . It can be seen that the electrical conductivity increases according to the following order:

S-CoCr > S-CoFe > S-NiCr > S-VCr (Unirradiated)
S*-CoCr > S*-NiCr > S*-CoFe > S*-VCr (Irradiated)

In spinel structure, the metal ions are located at two crystallographically different sites, the A site, comprising 8 tetrahedrally coordinated metal ions, and the B site, comprising 16 octahedrally coordinated metal ions. The Ni^{2+} ion preferentially occupy the B site (inverse spinel), whereas it is known that 80% of Mn^{2+} ions occupy the A site and 20% may go to the B site. The Zn^{2+} and Fe^{3+} ions are always in the A site. The Fe^{2+} and Fe^{4+} ions may occupy the B site . Co^{+2}, V^{5+} and Cr^{3+} may occupy both sites. For dc conductivity the charge carriers choose the easiest path between ions, but these paths might include some hops for which *R* "the distance between the ions" is large. The mixed valence ions present in B-sites are responsible for electrical conduction in ferrites. The conduction mechanism in ferrites is considered as the electron hopping between M^{2+} and M^{3+} at B sites (smaller distance than A sites). Therefore, the observed change in DC electrical conductivity with the change in sample composition may be attributed to a large extent to the change occurring in the M^{2+}/M^{3+} ratio in B sites (M i.e. metal ion).

Generally, the plots of $\ln\sigma_{d.c}$ vs. 1/T show the normal behavior character of a semiconductor which may be represented by Arrhenius dependence with more than one straight line in the temperature range of measurements. Each one of the different straight line segments in the ln σ–T^{-1} dependence in Fig. (8) obey the well known conventional law : $\sigma_{d.c} = \sigma_o \exp. (-E_{d.c} / kT)$, where σ_o is a constant , $E_{d.c}$ is the activation energy and k is the Boltzmann constant. [50]

The activation energy $E_{d.c}$ of each sample in the measured temperature range was determined from the slope of the linear plots using least squares methods and given in Table (5). The value of activation energy ranges from 0.02 to 1.25 eV. The compositional dependence of the activation energy evaluated from the slopes of the linear plots of DC electrical conductivity can be also observed from Table (5).

As mentioned above, the probability of electron hopping, which is primary between M^{2+} and M^{+3} states, is greater at the B sites due to smaller distances between the metallic ions at these sites. It is also observed that the activation energy obtained in the present work lie in the range of semiconductor, which suggests that the conduction is due to polaron hopping [9]. The hopping depends upon the activation energy, which is associated with the electrical energy barrier experienced by the electrons during hopping. One of the explanations for the observed change in activation energy with the change in the sample composition is based on the changes in ionic distances in the spinel ferrite crystal structure.

According to the above discussion it can be said that the electrical conduction mechanism can be explained in terms of the electron hopping model by Heikes and Johnson [3]. In other words, the conduction mechanism could be due to the electron hopping between two adjacent octahedral sites (B-sites) in the spinel lattice and a transition between $M^{2+} \leftrightarrow M^{3+}$ ions might take place [4]. It must be mentioned here that from orbital consideration the hopping mechanism between ions of different metal is more highly activated than that for ions of the same metal. [64].

The effect of γ-irradiation on the electrical properties of the studied ferrites has been also studied. The temperature dependence of DC- electrical conductivity for γ-irradiated samples is shown in Fig. (8). From this figure it can be observed that the conduction process of irradiated samples is similar to that of the unirradiated ones, especially at temperatures lower than 660˚K.The conductivity data are summarized and tabulated in Table (5). From the table, it is clear that the γ-irradiated ferrites showed an increase in the activation energy values except S-NiCr and a (decrease in the electrical conductivity except S-VCr) as compared with that found for the unirradiated ones.

The interaction of irradiation with solids depends on the type of radiation, the composition of solid itself, and the defects within it. It is generally accepted that ionizing radiation of solid produces mainly excitation and ionization, and may also cause a small amount of atomic or lattice displacement [65] .

The effect of γ– radiation on ferrites may cause the following interaction

$$\gamma + M^{n+} \rightleftharpoons M^{n+1} + e^{-} \qquad (17)$$

This reversible interaction leads to increase the amount of M^{n+} ions in the tetrahedral sites and in the same time decrease the ratio M^{n+} / M^{n+1} present in the octahedral sites. But the large distances between the ions present on tetrahedral sites prevent the effective contribution of these ions in the conduction process.

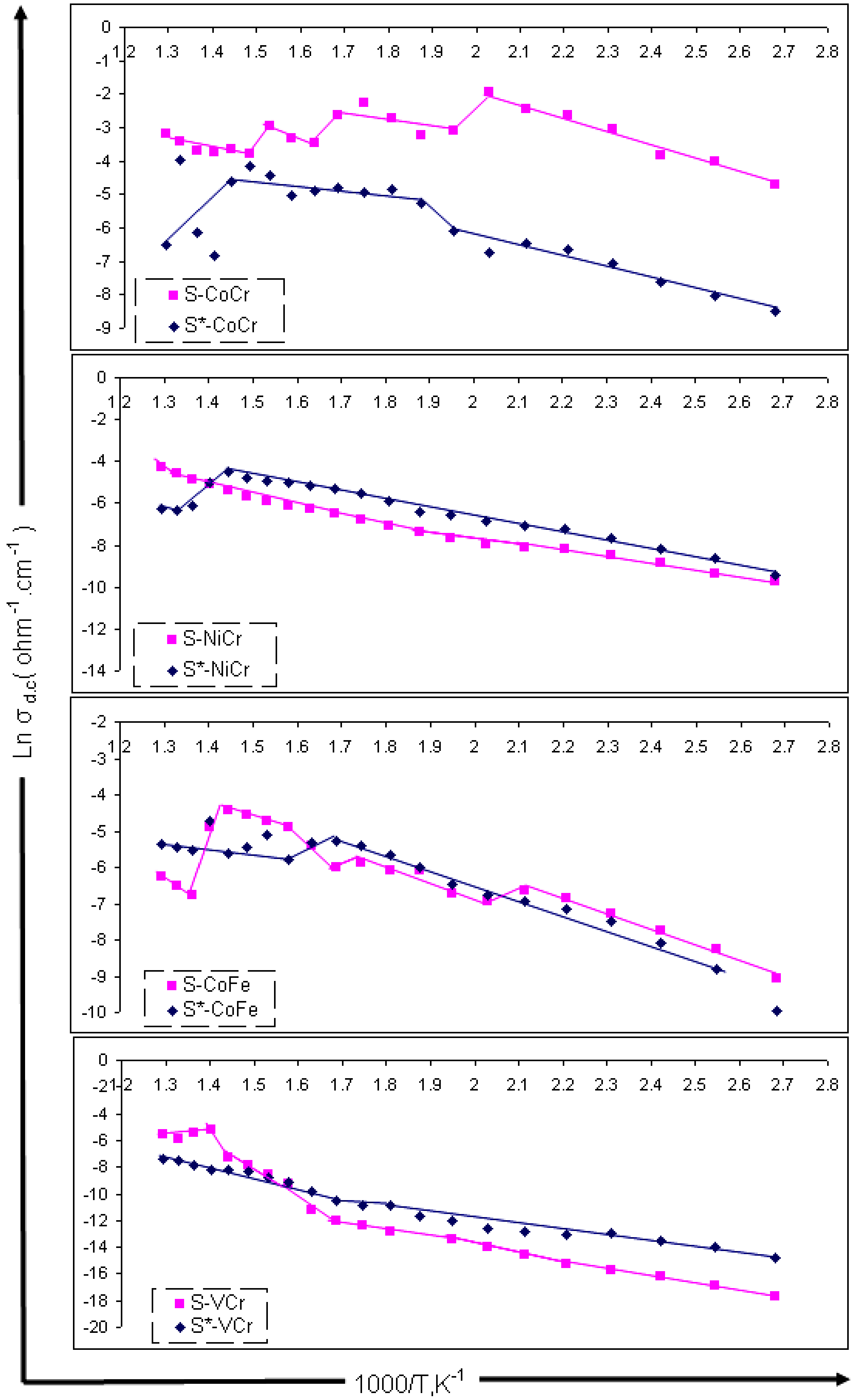

Fig. (8) Effect of temperature on DC electrical conductivity of Unirradiated and Irradiated Samples .

Table 5 : Activation energy of Unirradiated and irradiated Samples.

Composition	**σ_{dc} x10^{-6} at room temp. at 303 (˚K)**	**Temp. rang (˚K)**	**E_{dc} (ev)**	**T_b (˚K)**
S-CoCr	—	303 - 493	0.36	513
		533.573	0.66	593
		613 - 653	0.45	673
		673 - 773	0.24	
S*-CoCr	[—]	[313 - 673]	[0.35]	[673]
		[693 - 773]	[0.23]	
S-NiCr	7.33	303 - 493	0.27	493
		533 - 653	0.37	533
		673 - 773	0.60	653
		303-653	0.26	
S*-NiCr	[7.14]	[303-493]	[0.35]	[693]
		[303-693]	[0.93]	
S-CoFe	9.27	303 - 473	0.37	473
		493 - 573	0.34	573
		593 - 693	0.54	
S*-CoFe	[4.78]	[303 - 673]	[0.37]	[673]
		[713 - 773]	[0.02]	
S-VCr	0.01	303 - 613	0.39	613
		633 - 773	1.25	
S*-VCr	[1.28]	[303 - 593]	[0.343]	[593]
		[613 - 773]	[0.629]	

*[ ] Irradiated Sample.

5 - 2 AC-Results :-

Over a wide range of temperature from 300 up to 773 ^{o}K, the AC conductivity (σ_{ac}), dielectric constant (ε') and dielectric loss (ε'') were studied at different frequencies from 10^2 up to 10^6 Hz for all the investigated samples. The real part of the dielectric constant represents the capacitive behavior or polarizability of the material, while the imaginary part represents the energy losses due to polarization and conduction. The dielectric constant is a measure of the extent to which the electrical charge distribution in a material can be polarized by the application of an electrical field. In an alternating electric field, a sample is characterized by a complex dielectric constant (ε^*)

$$\varepsilon^* = \varepsilon' - j\,\varepsilon'' \qquad (6)$$

Where ε' and ε'' are the real and the imaginary of the complex dielectric constant, and j is the imaginary root of -1.

5 - 2 - 1 AC conductivity

The variations of $\sigma_{a.c}$ with temperature and frequency for all investigated samples are shown in Figs. 9(a-d). All the samples showed almost similar behavior in which the conductivity (in all samples except S-CoCr) increased with increasing temperature, especially at lower temperatures. In the low temperature region and in high temperature in case of S-NiCr , S-VCr, and S*-VCr the increase of $\sigma_{a.c}$ with temperature may be attributed to the increase in the drift mobility and hopping frequency of charge carriers with increasing temperature. Generally, it can be said that the studied samples shows a semi-conducting trend, as commonly seen in most ferrites.

The frequency dependence of conductivity at fixed temperature are shown in Figs.10 (a-d) . It can be seen that in most cases the conductivity $\sigma_{a.c}$ is slightly frequency dependent at lower frequencies. Whereas, as the frequency increases the conductivity becomes more and more frequency dependent. But by increasing the temperature, $\sigma_{a.c}$ independent on the frequency for a region of frequencies where the conductivity increases strongly with frequency, the transport is dominated by contributions from hopping infinite clusters. Finally, the region where the high frequency cut off starts to play a role (here saturation will be reached) is encountered.

The dispersion in the AC electrical conductivity of polycrystalline ferrites was explained on the basis of interfacial polarization that formed due to the inhomogeneous structure of ferrite material. Generally, for all samples, dispersion of the AC conductivity decreases with increasing the temperature. At relatively high temperatures are shown in figs 9(a-d), the AC conductivity seems to be frequency independent until a certain frequency at which the conductivity begins to decrease. As mentioned before, at this frequency the applied field obstructs hopping conduction. [50]

Similar to our observation, frequency dependence of AC conductivity has been explained in the past with the help of Maxwell–Wagner (MW) – two-layer model or the heterogeneous model of the polycrystalline structure of ferrites (Koop's 1951). According to MW theory two layers form a dielectric structure. The first layer consists of ferrite grains of fairly well conducting (divalent metal ions), which is separated by a thin layer of poorly conducting substances, which forms the grain boundary. These grain boundaries are more active at lower frequencies; hence the hopping frequency of electron between M^{2+} and M^{3+} ion is less at lower frequencies. As the frequency of the applied field increased the conductive grains became more active by promoting the hopping of electron between M^{2+} and M^{3+} ions, thereby increasing the hopping frequency. They observed a gradual increase in conductivity with frequency but at higher frequencies the frequency of hopping between the ions could not follow the applied field frequency and it lagged behind it . This causes a dip in conductivity at higher frequencies [66] .

Aguilar-Hernandez and Potje-Kamloth (2001) and Singh (1991) accounted for the frequency dependent conductivity behaviour due to two mechanisms expressed as

$$\sigma(\omega) = \sigma_{a.c.}(\omega) + \sigma_{d.c.} \qquad (18)$$

The above equation represents the total conductivity in the context of the theory of relaxation processes in dielectric materials (Jonscher 1976, 1983). The main idea relies on the separate processes. The total measured conductivity at a given frequency is separated into $\sigma_{a.c.}(\omega)$ and $\sigma_{d.c.}$ This is simply the limit of $\sigma_{a.c.}(\omega)$ when $\omega \sim 0$. From figs.10(a-d) it is evident that at lower frequency, conductivity is independent of frequency but may be dependent on temperature [67].

A common feature of all semiconductor materials is the frequency dependent conductivity $\sigma_{a.c.}(\omega)$, i.e.

$$\sigma_{a.c.}(\omega) = \sigma(\omega) - \sigma_{d.c.} = A\omega^{s} \qquad (19)$$

Where $\sigma_{d.c.}$ is the DC part of the total conductivity σ, A is a constant and ($s \leq 1$) is the frequency exponent. The phenomenon has variously been ascribed to the relaxation caused by the motion of electrons or atoms, hopping or tunneling, between the equilibrium sites. [50]. The exponent *s* is determined from the experimental data in figs.10 (a-d) using the equation:-

$$[s = d(\mathrm{Ln}\,\sigma_{a.c.}(\omega)) / d(\mathrm{Ln}(\omega))] \qquad (20)$$

The values obtained are listed in Table (6). It can be seen that, the values of the exponent *s* lie between 0.001 to 0.588 and decreases with increasing temperature for all the samples under investigation [50]. Also the values of *s* for irradiated samples is lower than that of unirradiated ones. The obtained results agree well with the results of similar systems [68,69].

It is known that the behaviour of s with the temperature can be taken as a criterion of the conduction mechanism [23,24]. If *s* increases with temperature, a small polaron is the predominant mechanism, while the large overlap polaron is characterized by a minimum followed by increase of s with further increase of the temperature. In the case where s is temperature-independent, the quantum mechanical tunneling is expected and the correlated barrier hopping is usually associated with decreasing of s with the temperature.

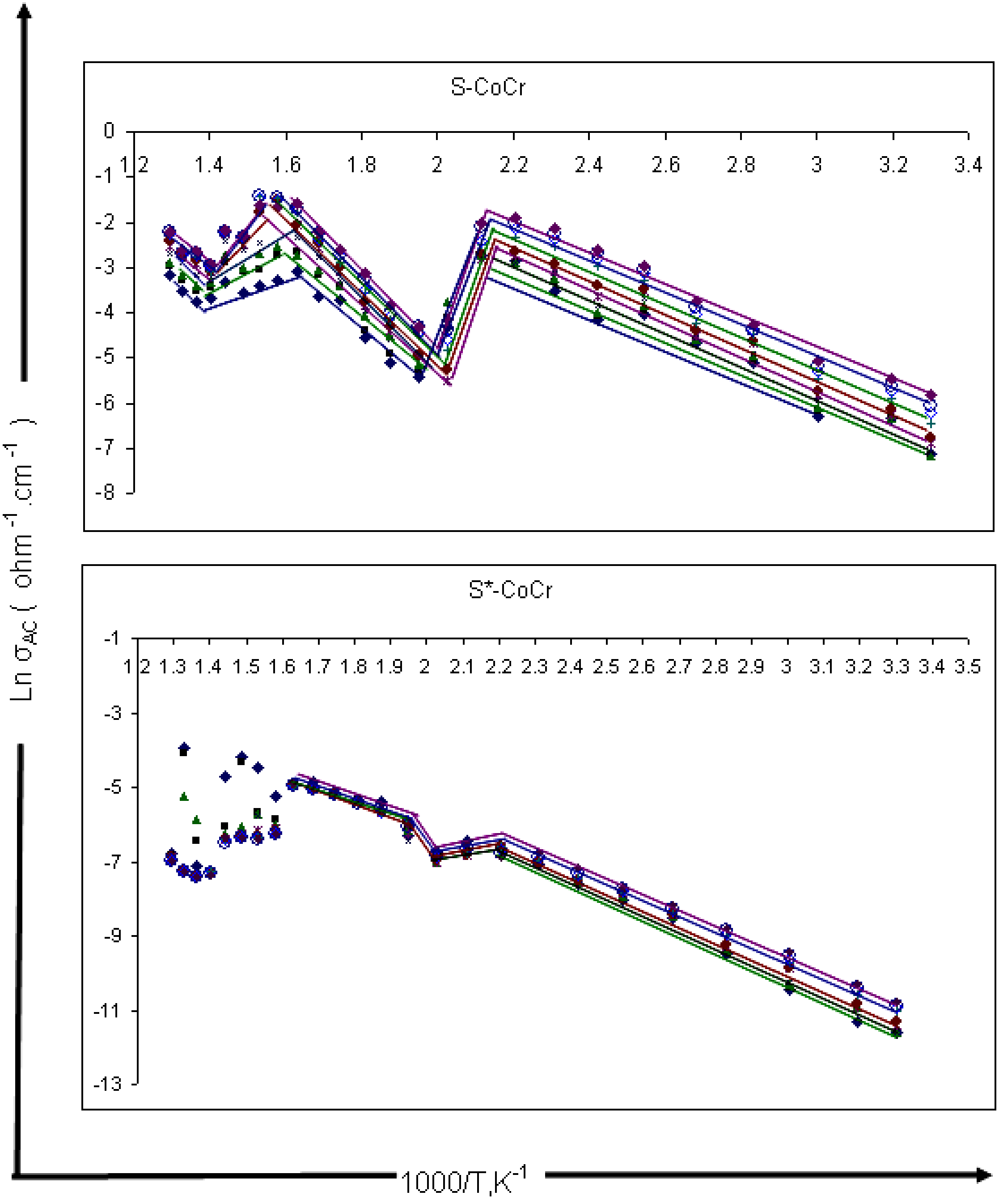

Fig. (9 - a) Effect of temperature on AC electrical conductivity of (S-CoCr) Unirradiated and (S*-CoCr) Irradiated Spinel .

◆ 100Hz ■ 500Hz ▲ 1KHz × 10KHz ✱ 50KHz
◆ 100KHz + 300KHz ◇ 500KHz ◇ 700KHz ◆ 1MHz

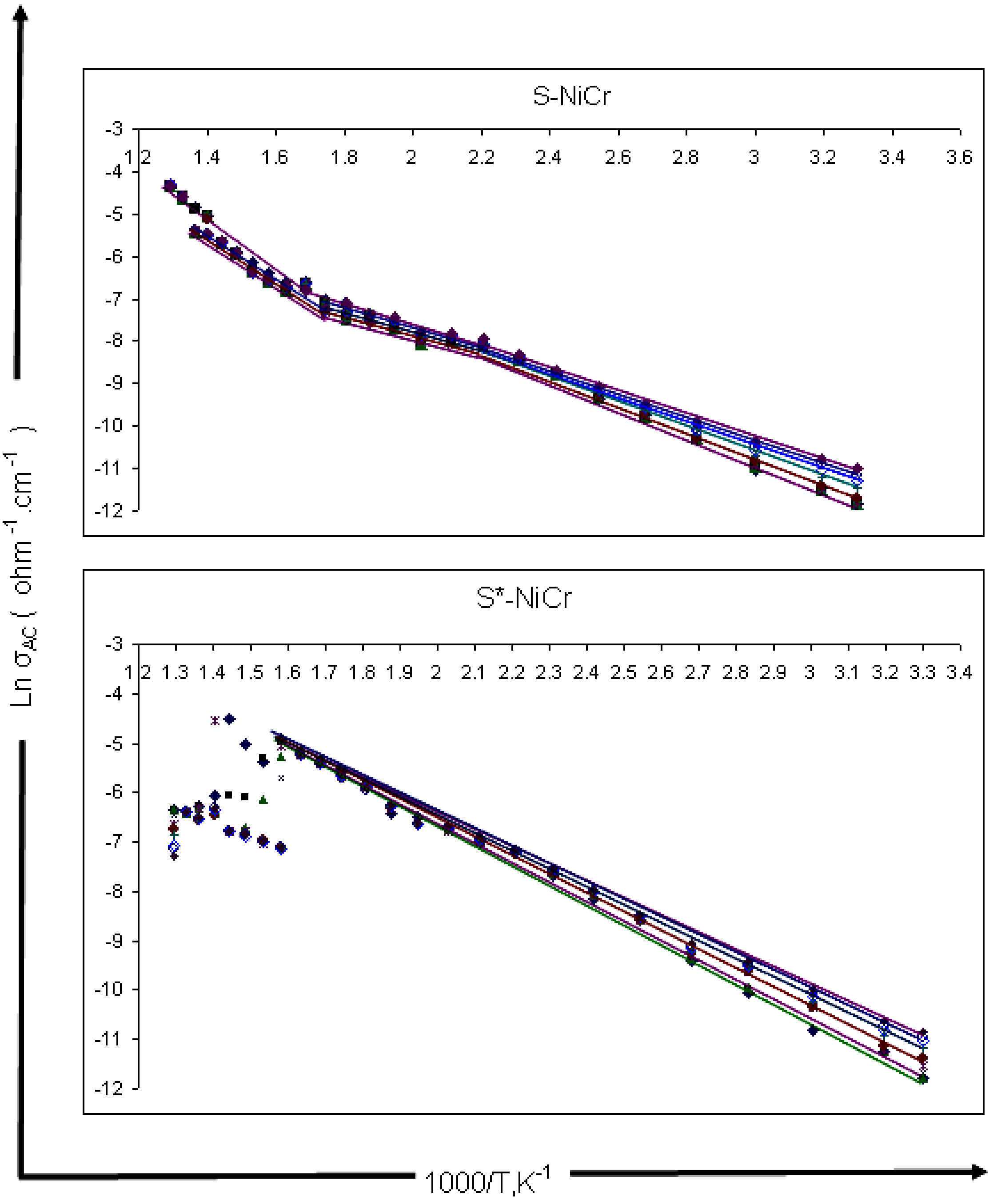

Fig. (9 - b) Effect of temperature on AC electrical conductivity of (S-NiCr) Unirradiated and (S*-NiCr) Irradiated Spinel.

◆ 100Hz	■ 500Hz	▲ 1KHz	× 10KHz	✳ 50KHz
● 100KHz	+ 300KHz	◇ 500KHz	○ 700KHz	◆ 1MHz

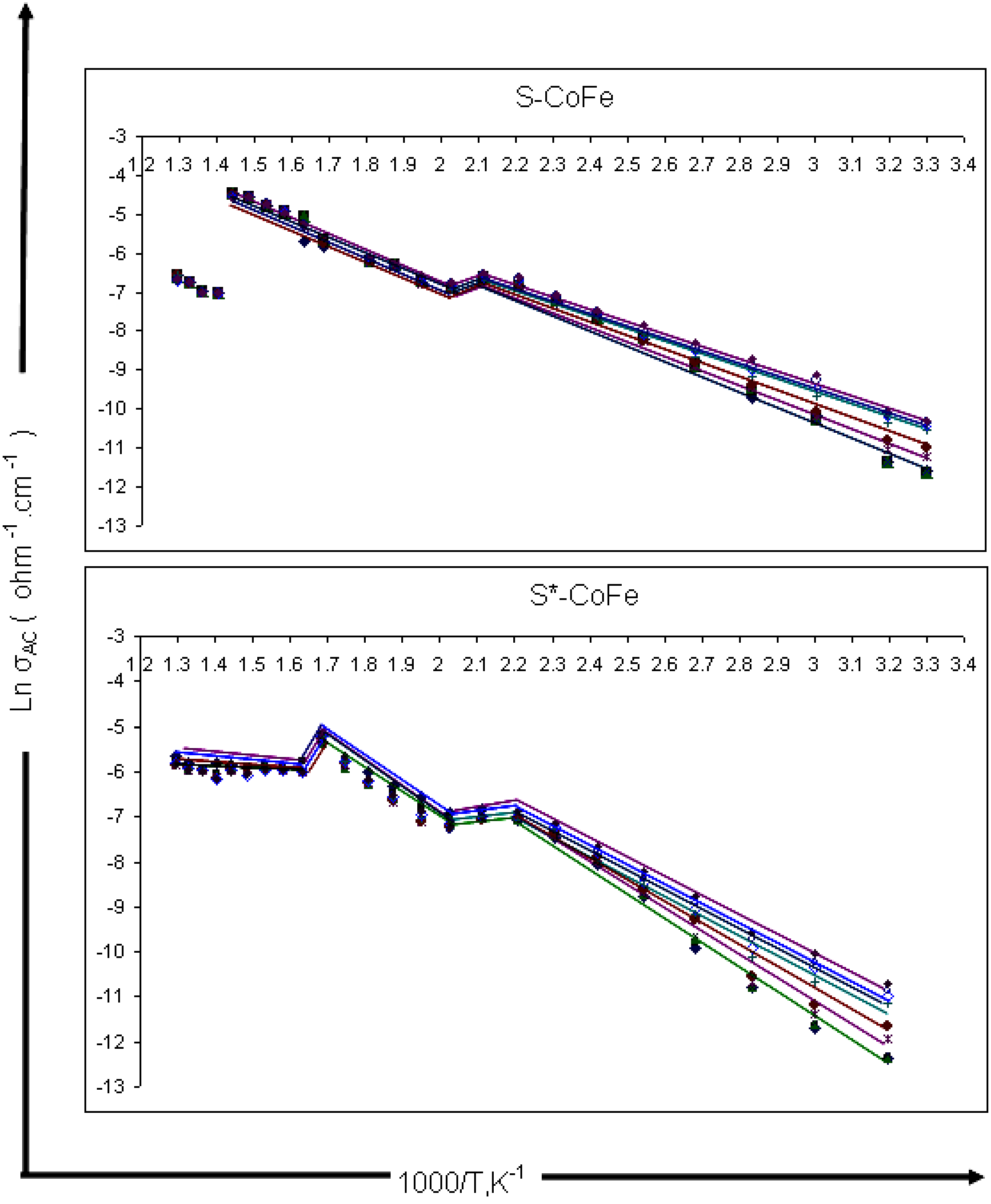

Fig. (9- c) Effect of temperature on AC electrical conductivity of (S-CoFe) Unirradiated and (S*-CoFe) Irradiated Spinel.

◆ 100Hz ■ 500Hz ▲ 1KHz × 10KHz ✱ 50KHz
◆ 100KHz + 300KHz ◇ 500KHz ◇ 700KHz ◆ 1MHz

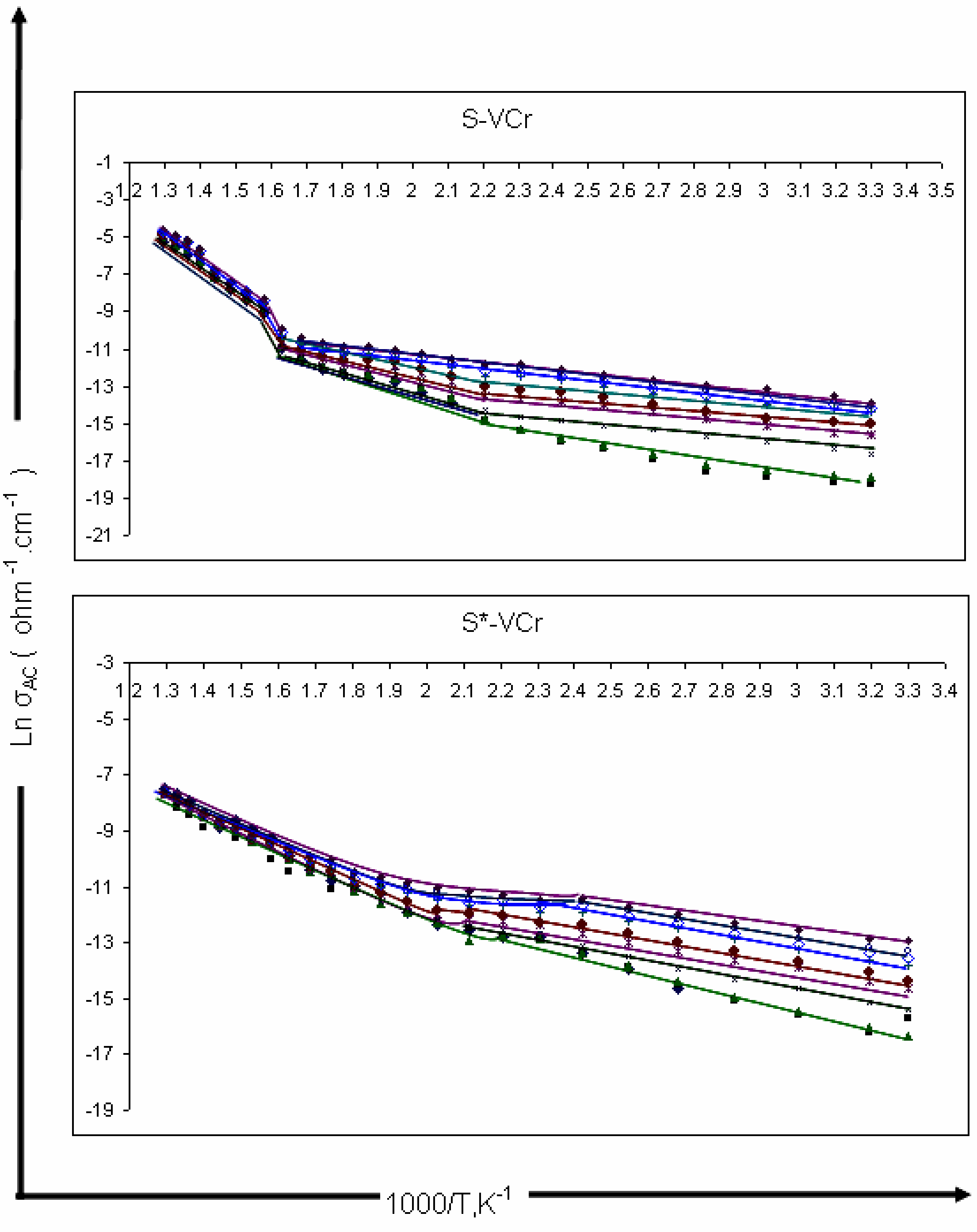

Fig. (9- d) Effect of temperature on AC electrical conductivity of (S-VCr) Unirradiated and (S*-VCr) Irradiated Spinel.

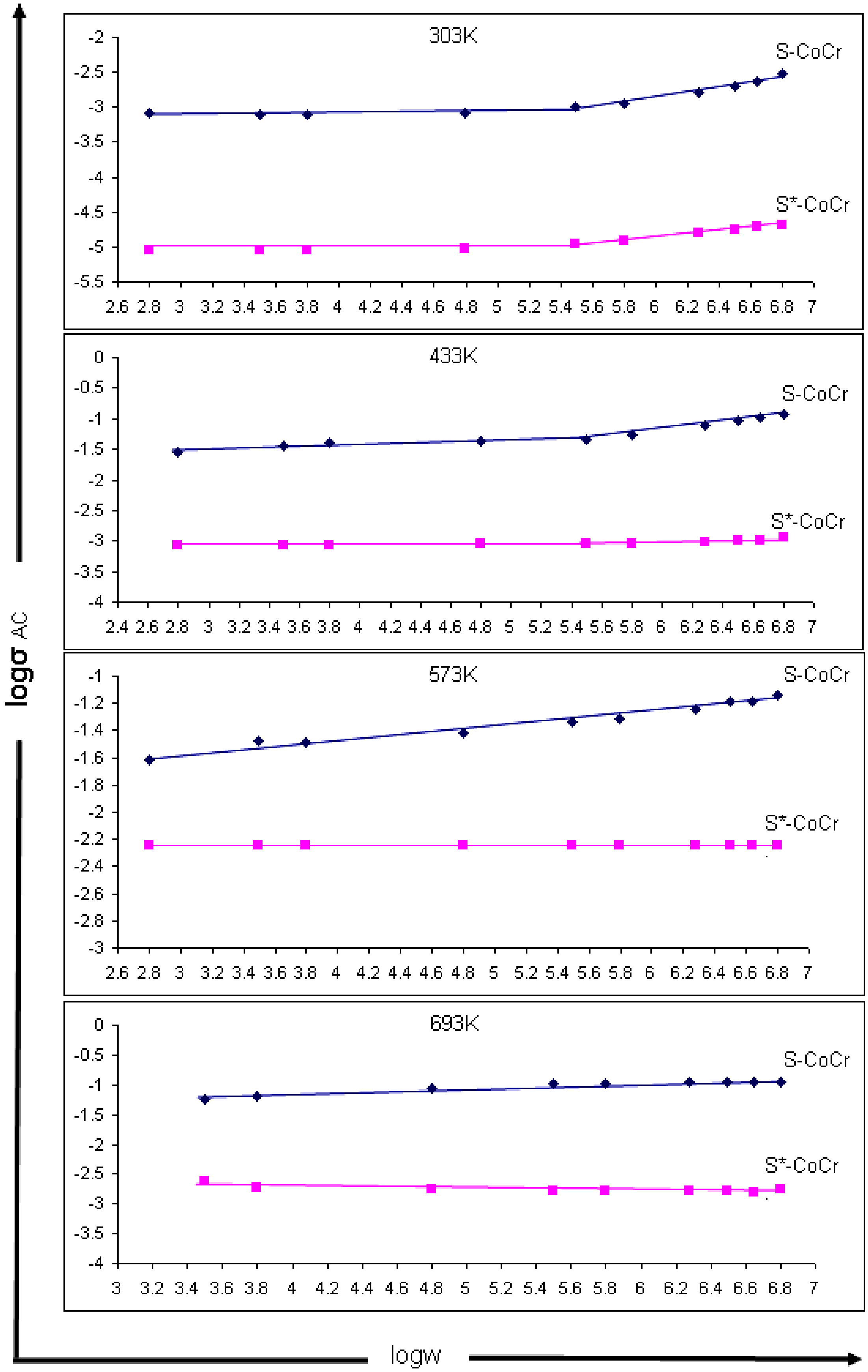

Fig. (10- a) Effect of frequency on AC electrical conductivity of (S-CoCr) Unirradiated and (S*-CoCr) Irradiated Spinel.

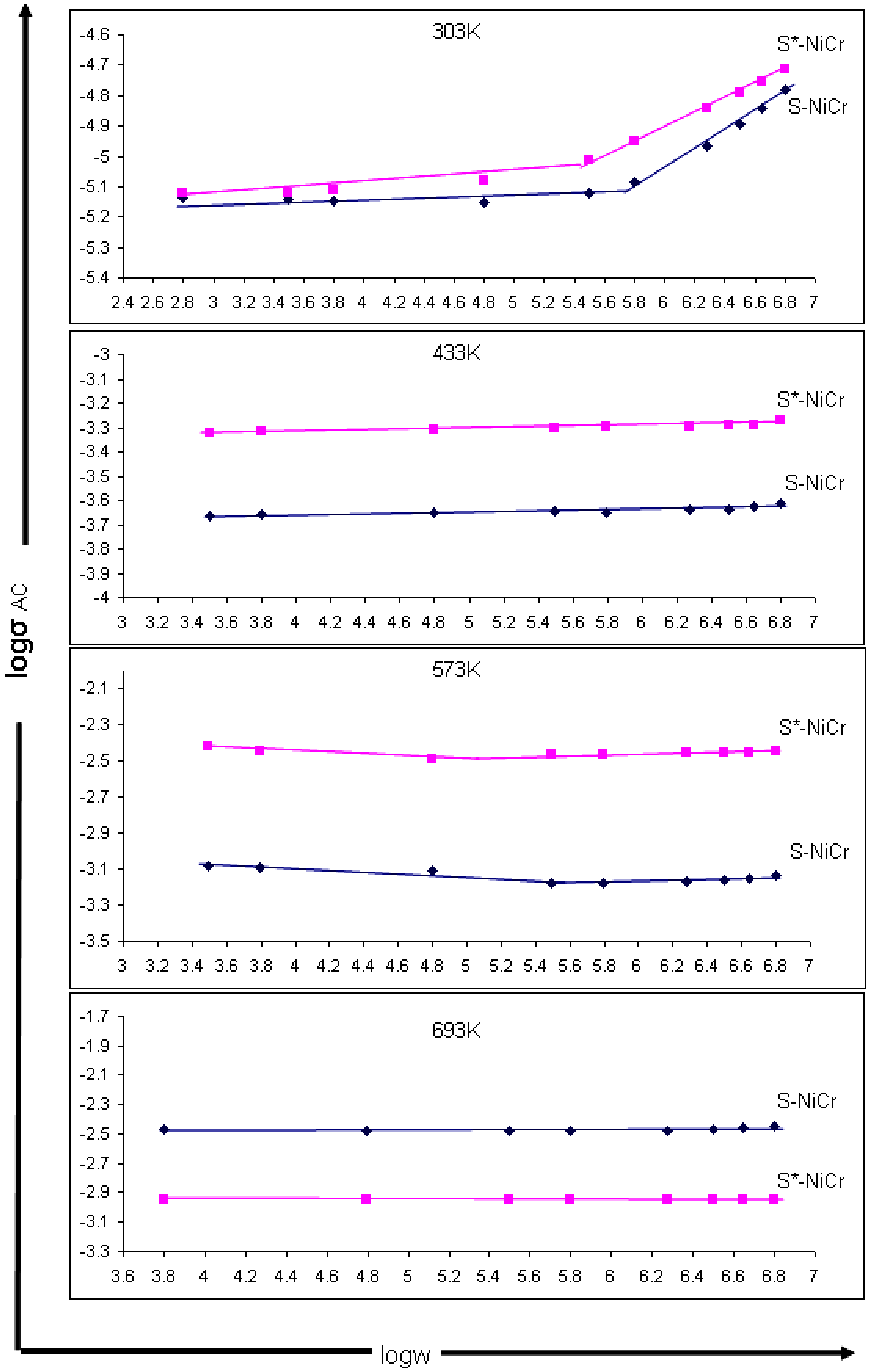

Fig. (10- b) Effect of frequency on AC electrical conductivity of (S-NiCr) Unirradiated and (S*-NiCr) Irradiated Spinel.

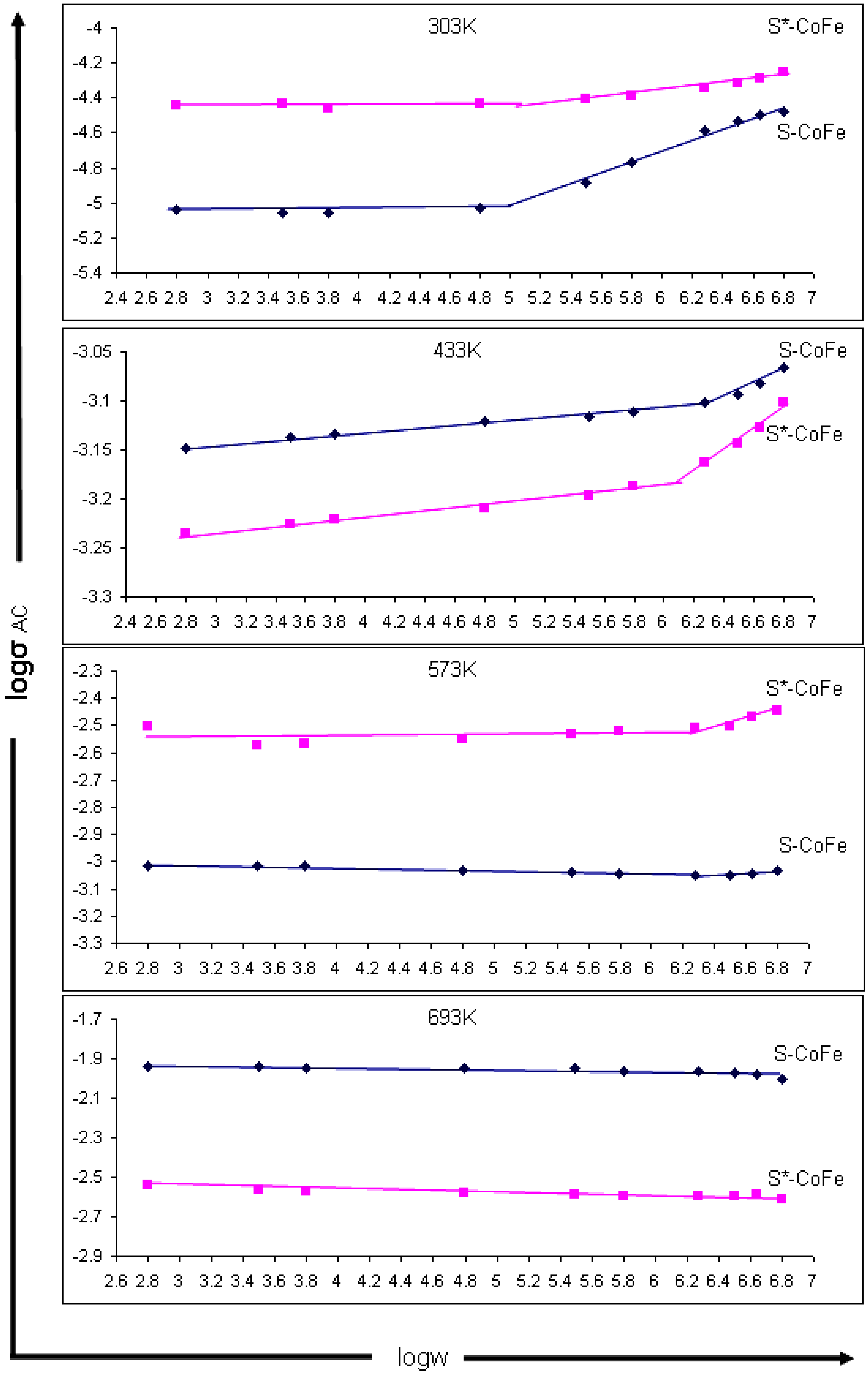

Fig.(10- c) Effect of frequency on AC electrical conductivity of (S-CoFe)Unirradiated and (S*-CoFe) Irradiated Spinel.

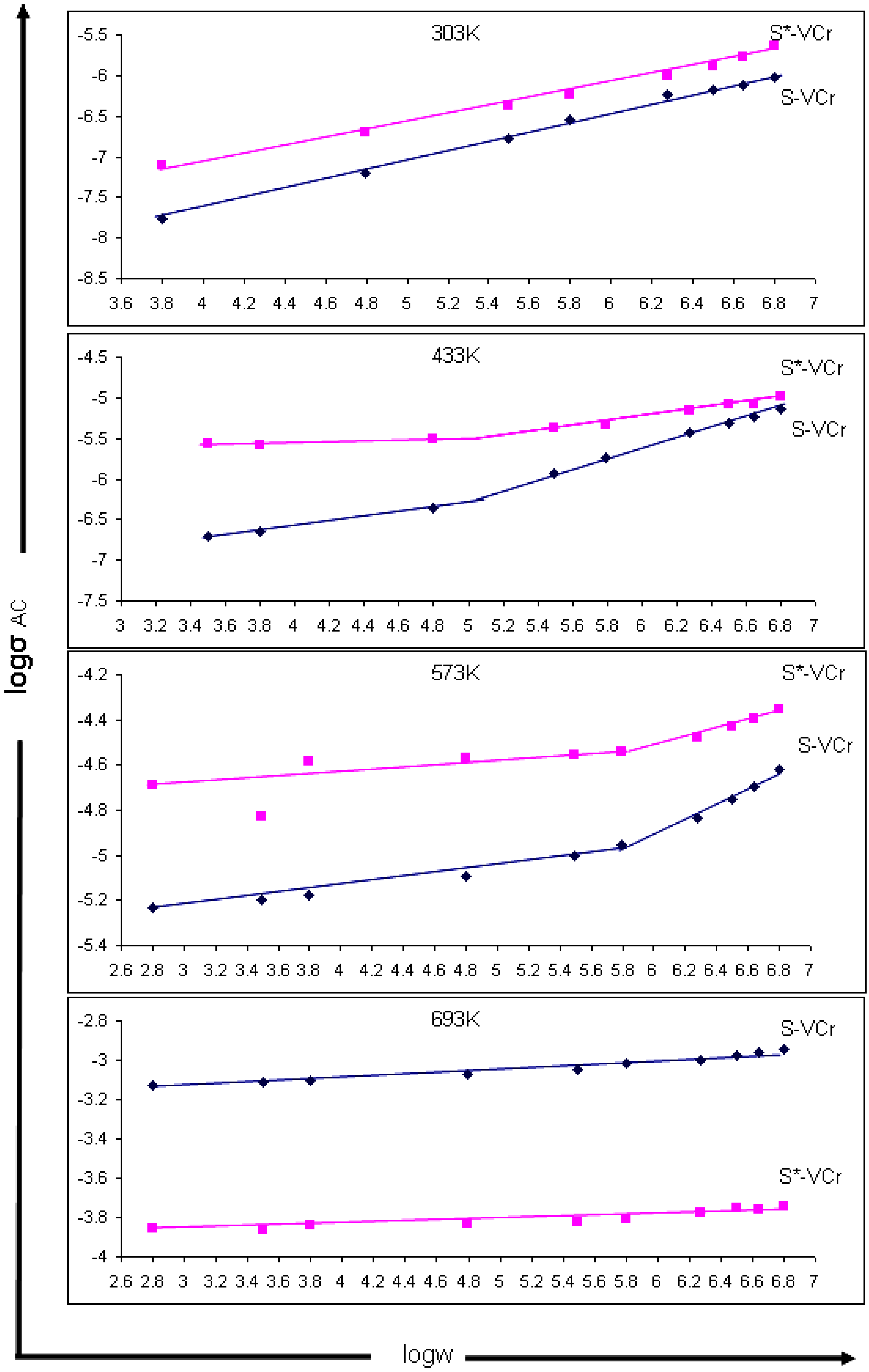

Fig. (10- d) Effect of frequency on AC electrical conductivity of (S-VCr) Unirradiated and (S*-VCr) Irradiated Spinel.

Table 6 : Dimensionless parameter of Unirradiated and irradiated Samples.

Composition	Temp.(˚K)	Freq .rang	S
S-CoCr	303	100Hz-1MHz	0.134
	433	100Hz-1MHz	0.139
	573	100Hz-1MHz	0.106
	693	100Hz-1MHz	0.110
S*-CoCr	[303]	[100Hz-1MHz]	[0.092]
	[433]	[100Hz-1MHz]	[0.022]
	[573]	[100Hz-1MHz]	[0.001]
S-NiCr	303	100KHz-1MHz	0.301
	433	100Hz-1MHz	0.011
	573	50KHz-1MHz	0.028
	693	50KHz-1MHz	0.019
S*-NiCr	[303]	[100Hz-1MHz]	[0.104]
	[433]	[100Hz-1MHz]	[0.012]
	[573]	[50KHz-1MHz]	[0.013]
	[693]	[50KHz-1MHz]	[0.001]
S-CoFe	303	100Hz-1MHz	0.159
	433	100Hz-100KHz	0.012
	433	300KHz-1MHz	0.066
	573	500KHz-1MHz	0.055
S*-CoFe	[303]	[100Hz-1MHz]	[0.045]
	[433]	[100Hz-1MHz]	[0.028]
	[573]	[100Hz-1MKHz]	[0.019]
S-VCr	303	500Hz-1MHz	0.588
	433	500Hz-1MHz	0.494
	573	100Hz-100KHz	0.094
	573	300KHz-1MHz	0.400
	693	100Hz-1MHz	0.022
S*-VCr	[303]	[100Hz-1MHz]	[0.398]
	[433]	[100Hz-1MHz]	[0.148]
	[573]	[100Hz-1MHz]	[0.086]
	[693]	[100Hz-1MHz]	[0.029]

* [ ] Irradiated Sample.

The frequency exponent *s* found to be decrease with increasing temperature, which indicates that the correlated barrier hopping (C.B.H.) is the most probable mechanism in our samples [50].

The experimental data of the ac conductivity of the investigated ferrite successfully comply with the following equation: -

$$\sigma_{a.c} = \sigma_0 \, e^{(Ea.c / kT)} \quad (21)$$

Where σ_0 is a temperature-dependent term and $E_{a.c}$ represents the activation energy of conduction mechanism. The other parameters have their usual meaning. The values of $E_{a.c}$ for each composition, over the same range of temperature were calculated at different frequencies. The obtained values of $E_{a.c}$ are tabulated in Table (7) .The influence of temperature on AC conductivity has been explained by considering the mobility of charge carriers responsible for hopping. As temperature increases the mobility of hopping ions also increases thereby increasing conductivity [67] .In general, the activation energy is found to decrease with increasing frequency for the studied ferrite. As mentioned above, in the DC conductivity the charge carriers choose the easiest path between the ions. These paths will include some jumps for which R, the distance between the ions, is large. This is not so important in the AC conduction. Thus low activation energy may be involved in the AC conduction. The difference between the activation energies of $\sigma_{d.c}$ and $\sigma_{a.c}$ may be attributed to the effective drop of the electric field within the bulk due to the presence of space charge accumulations at the electrodes which were noticed in DC-measurements [70 , 71].

Table 7 : Activation energy of Unirradiated and irradiated Samples.

Composition	**Temp. rang (°K)**	**$E_{a.c}$ (ev) at 1MHz**	**T_b (°K)**
S-CoCr	303-473	0.306	493
	493-613	0.606	633
	633-773	0.287	
S*-CoCr	[303-473]	[0.313]	[493]
	[493-613]	[0.398]	[633]
	[633-673]	[0.055]	[693]
	[963-773]	[0.317]	
S-NiCr	303-613	0.233	633
	633-673	0.436	693
	733-773	1.28	
S*-NiCr	[303-613]	[0.297]	[633]
	[633-713]	[0.339]	[733]
	[733-773]	[0.725]	
S-CoFe	303-473	0.28	413
	493-533	0.233	553
	573-693	0.777	693
	713-773	0.333	
S*-CoFe	[303-613]	[0.258]	[633]
	[633-713]	[0.093]	[733]
	[733-773]	[0.225]	
S-VCr	303-493	0.174	493
	513-613	0.261	633
	633-773	1.22	
S*-VCr	[303-613]	[0.16]	[633]
	[633-773]	[0.533]	

*[ ] Irradiated Sample.

5 - 3 Dielectric constant (ε′)

The complex dielectric constant ε* is represented by

$$\varepsilon^*=\varepsilon'-j\varepsilon'' \qquad (6)$$

where the real part (dielectric constant) ε′ describes the stored energy and the imaginary part (dielectric loss) ε″ describes the dissipated energy .The dielectric properties of polycrystalline ferrites are dependent on several factors such as the method of preparation and substitution of different ions in the ferrites[53]. Figs. 11(a-b) shows the variation of dielectric constant with frequency from 10^2 Hz to 1 MHz. It can be seen that all the samples show the frequency-dependent phenomena i.e. the dielectric constant decreases with increasing frequency. This is a normal behavior observed in most of the ferrimagnetic materials, which may be due to the interfacial polarization as predicted by Maxwell–Wagner [11]. According to Maxwell–Wagner model, the dielectric structure of a ferrite material is assumed to be made up of two layers. First layer being a conducting layer consists of large ferrite grains and the other being the grain boundaries that are poor conductors. According to Rabinkin and Novikova [12] the polarization in ferrites is through a mechanism similar to the conduction process. By electron exchange between M^{n+} and M^{n+1}, the local displacement of electrons in the direction of the applied field occurs and these electrons determine the polarization. The polarization decreases with increasing frequency and then reaches a constant value due to the fact that beyond a certain frequency of external field, the electron exchange between M^{n+} and M^{n+1} cannot follow the alternating field.

The results of dielectric relaxation intensity $\Delta\ \varepsilon'$ (i.e. the difference between the values of the dielectric constant at low and high frequencies) are displayed as a function of temperature for each sample in Figs.12(a-d). It is shown that $\Delta\ \varepsilon'$ slight effect at lower frequencies, but increases at higher frequencies with increasing the temperature for all compositions. Fig.(13-a) correlates the dielectric constant (ε') and temperatures at different fixed frequencies. From the figure, it is clear that the general trend is the increase of ε' with increasing frequency. It is also clear that with increasing temperature up to a certain value depends on the sample composition (443-500 °K), ε' is more or less constant. The slow variation of the dielectric constant (ε') with temperature is a general trend in ionic solids [25]. It may be due to space charge polarization caused by impurities or interstitial in materials which leads to that ε′ it is independent of temperature. Moreover, in narrow band semi-conductors, the charge carriers are not free to move but are trapped causing a polarization, and also the thermal energy given at this range of temperature to the samples was not sufficient to free the localized dipoles to be oriented in the field direction. By increasing temperature above the range in which ε′ is temperature independent, the number of charge carriers increases exponentially and thus produce further space charge polarization and hence leads to an increase in the dielectric constant (ε′). In addition, as the temperature increases, the thermal energy librates more localized dipoles and the field tries to align them in its direction either by rotational or orientational motion contributing to an increase in ε′ up to the maximum value, after which the thermal energy added to the system with electrical energy of the field decreases the internal viscosity, instantly, giving more degrees of freedom leading to a disturbance in the system and hence decreasing ε′ again up to inverse peak value. By more increasing in temperature the disturbance will be decreased and the localized dipoles alignment will be reached again and hence ε′ will be increases.

In general, for the high temperature range, the saturation in the generation of charge carriers was reached. Therefore, the electronic exchange (M^{2+} / M^{3+}) cannot follow the field variation and hence the dielectric constant ε′ decrease. It was found that ε′ reached maximum value at low temperature with high frequency and at high temperature with low frequency.

The reason for the high abnormally values of dielectric constant ,ε′, may be attributed to the Maxwell - Wagner interfacial polarization .This suggested that, the simplest form of interfacial effect is represented by a capacitive layer as a result of the formation of barrier between the electrode and the bulk material. Additionally, the presence of different phases in the bulk material may also form barriers. These barriers are less conducting than the bulk materials of the samples. [37]

The temperature and frequency dependence of the dielectric constant (ε′) for γ -irradiated ferrites are shown in Fig.(13-b) . The behaviors are similar to that observed for unirradiated samples until 533˚K , because behind this temperature no data shown except the samples S-CoFe, S*- CoFe have some data. The ε′ values for irradiated samples are higher than that of unirradiated ones. The observed increase in ε′ values by irradiation may be attributed to a gradual formation of more charge carriers or easily orient able dipolar molecules that are capable of conducting the electric current. It is presumed that these charge carriers or dipolar molecules were formed from composition and structural modifications (oxidation - reduction process as mentioned above) caused by irradiation.

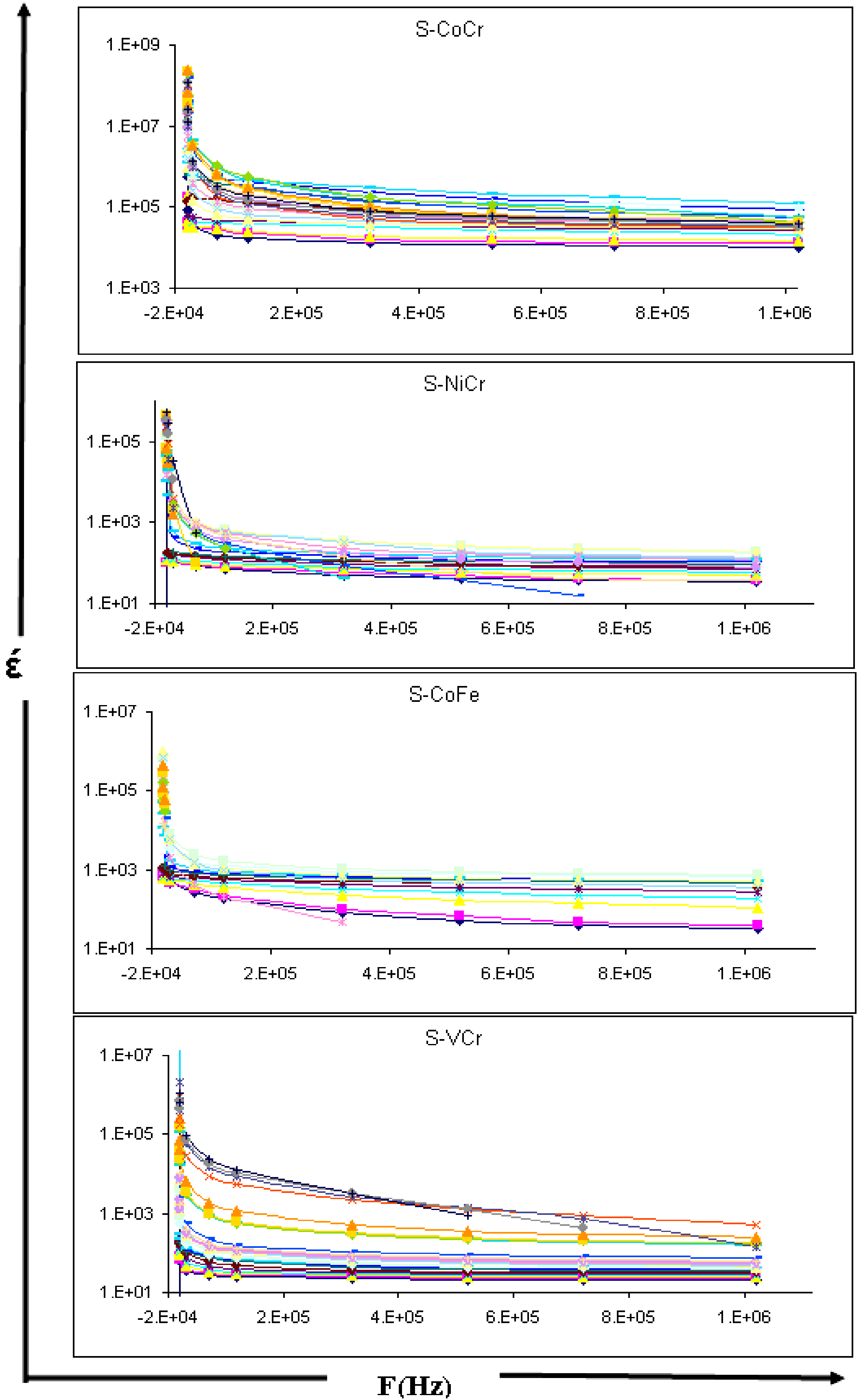

Fig.(11-a)Variation of dielectric constant with frequency of Unirradiated Spinel.

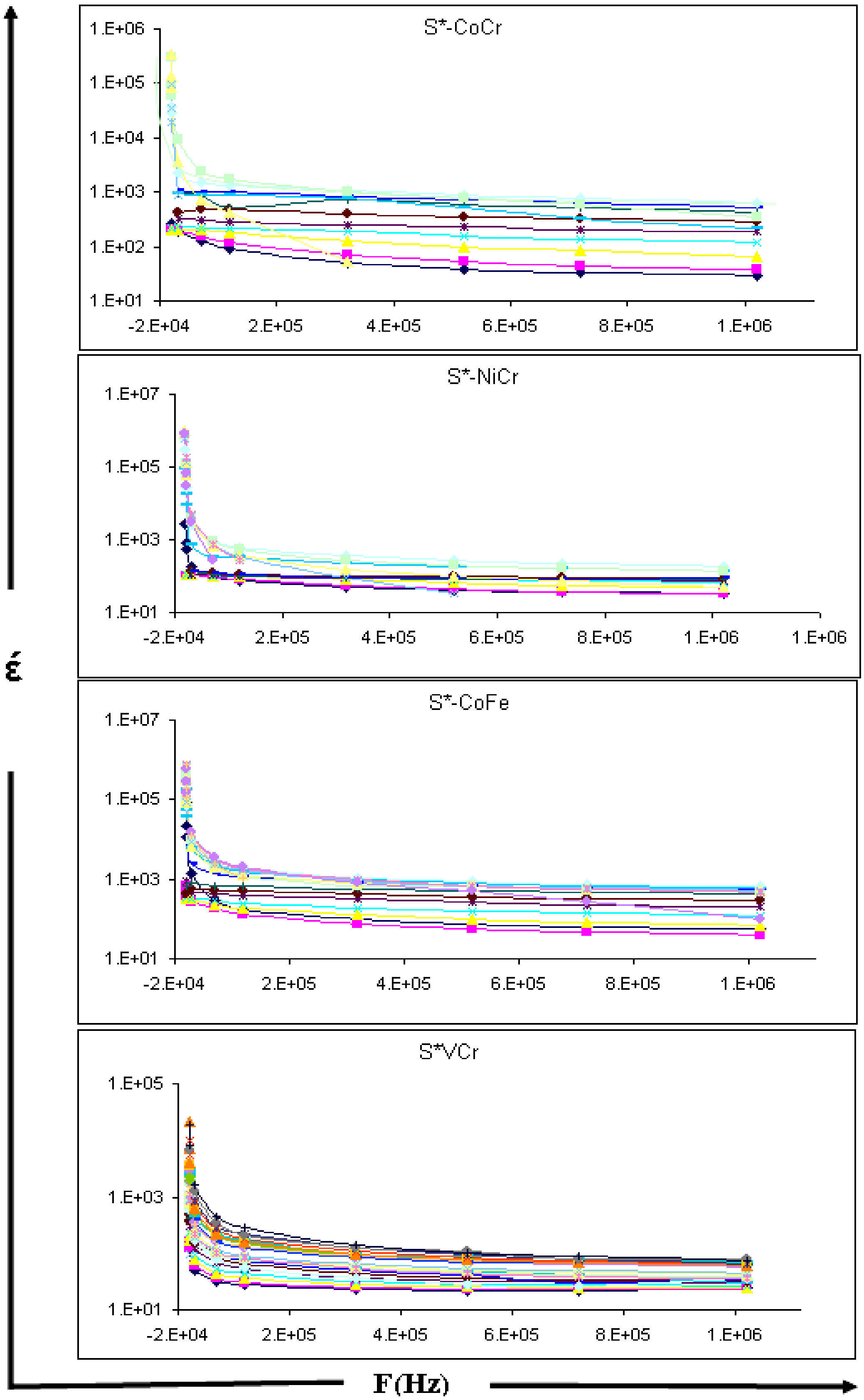

Fig.(11-b)Variation of dielectric constant with frequency of Irradiated Spinel.

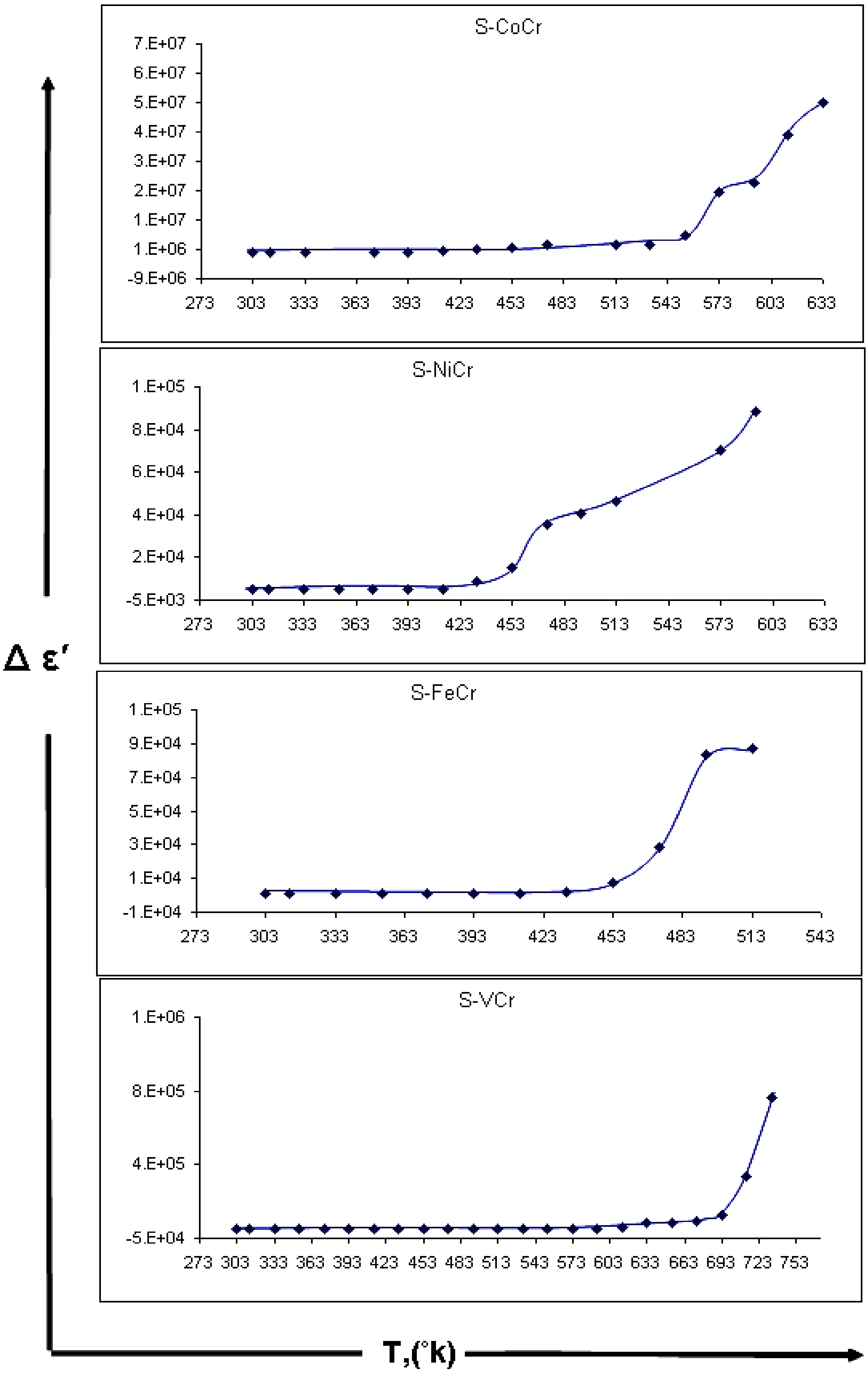

Fig.(12-a)Dielectric relaxation intensity($\Delta \varepsilon'$) as a function of temperature of Unirradiated Spinel.

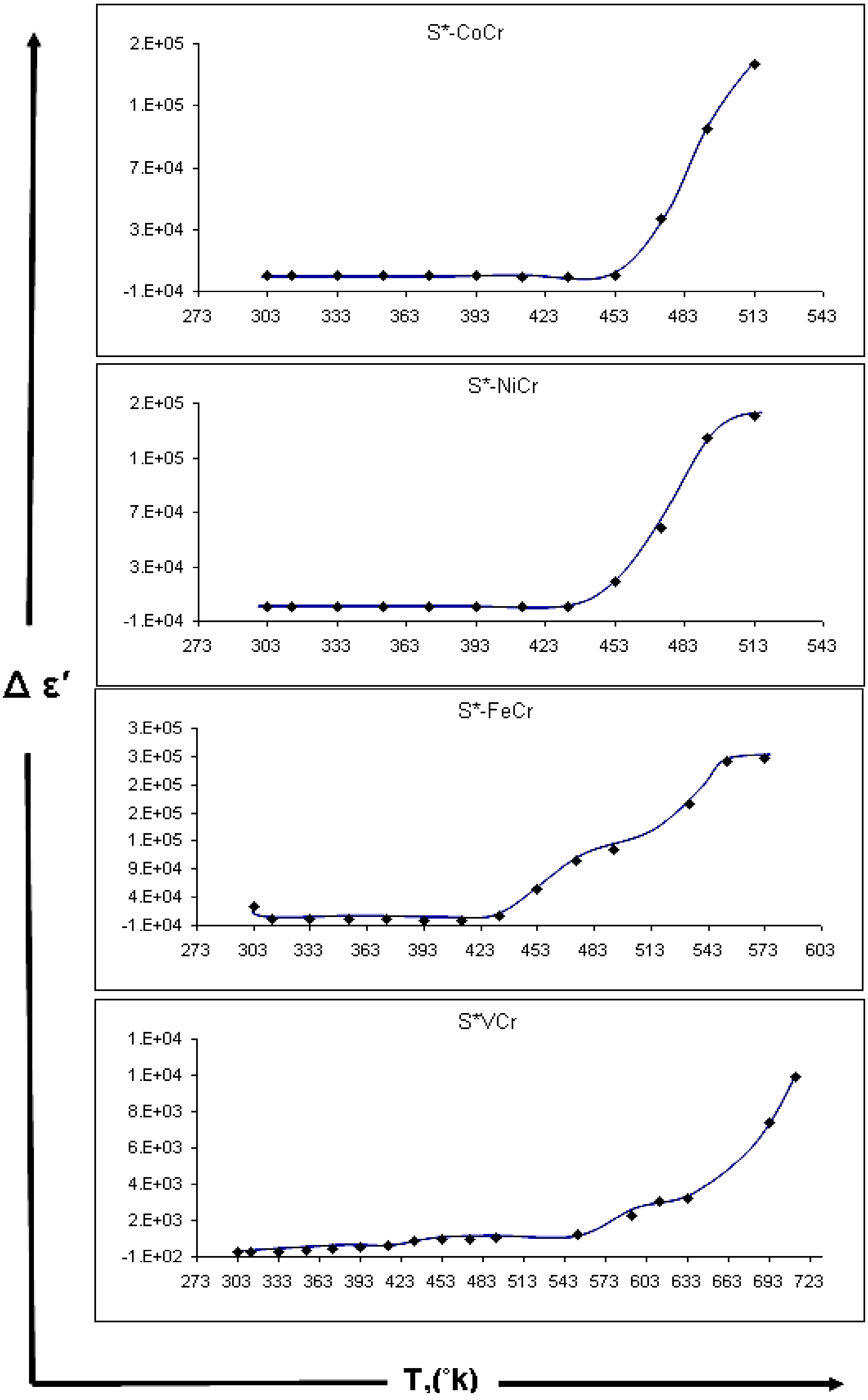

Fig.(12-b)Dielectric relaxation intensity(Δ ε') as a function of temperature of Irradiated Spinel.

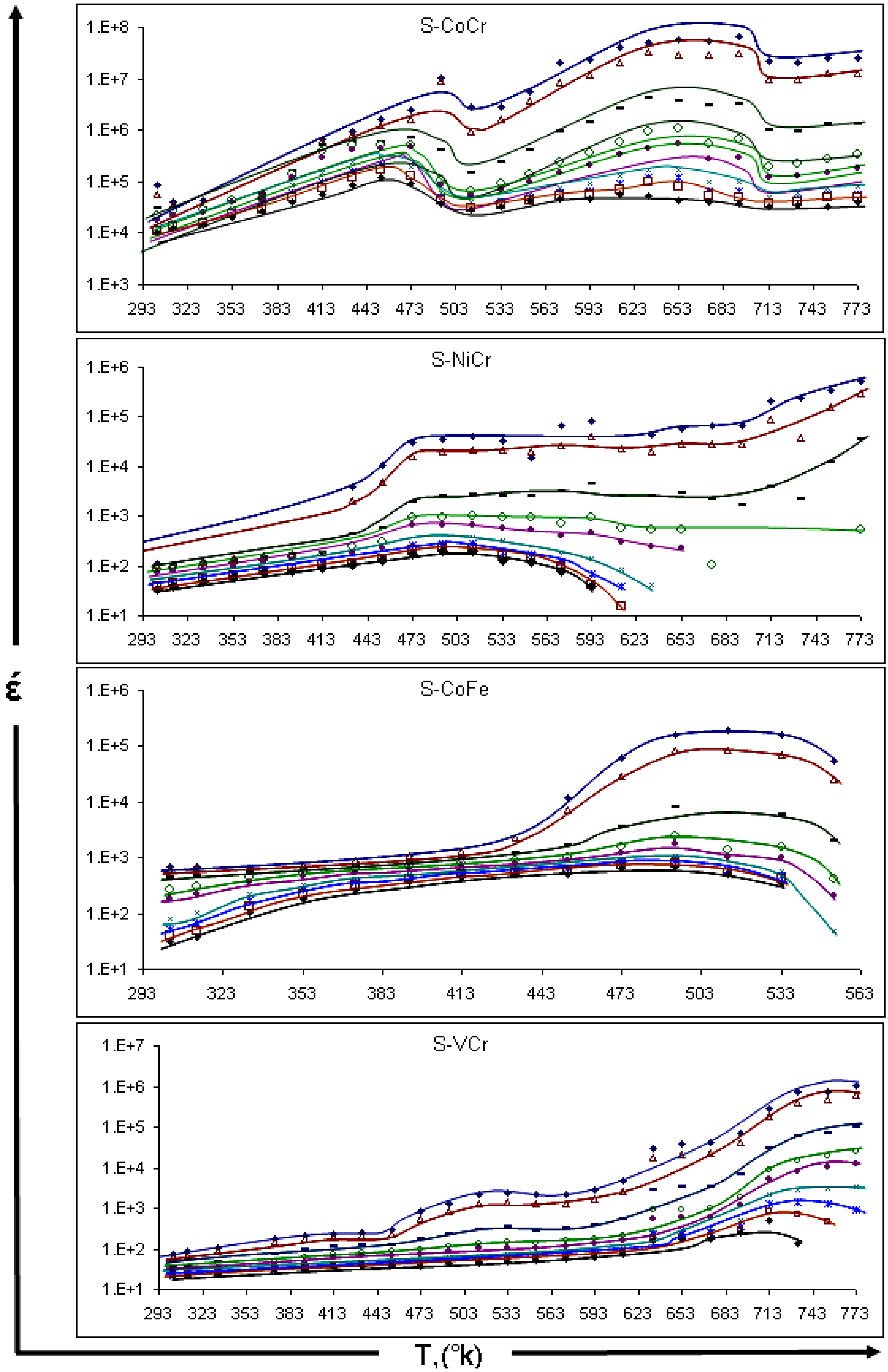

Fig .(13-a) Effect of frequency and temperature on dielectric constant (ε′) for unirradiated samples. Where

◆ 500Hz △ 1KHz ▬ 10KHz ○ 50KHz ● 100KHz × 300KHz ✱ 500KHz □ 700KHz ◆ 1MHz

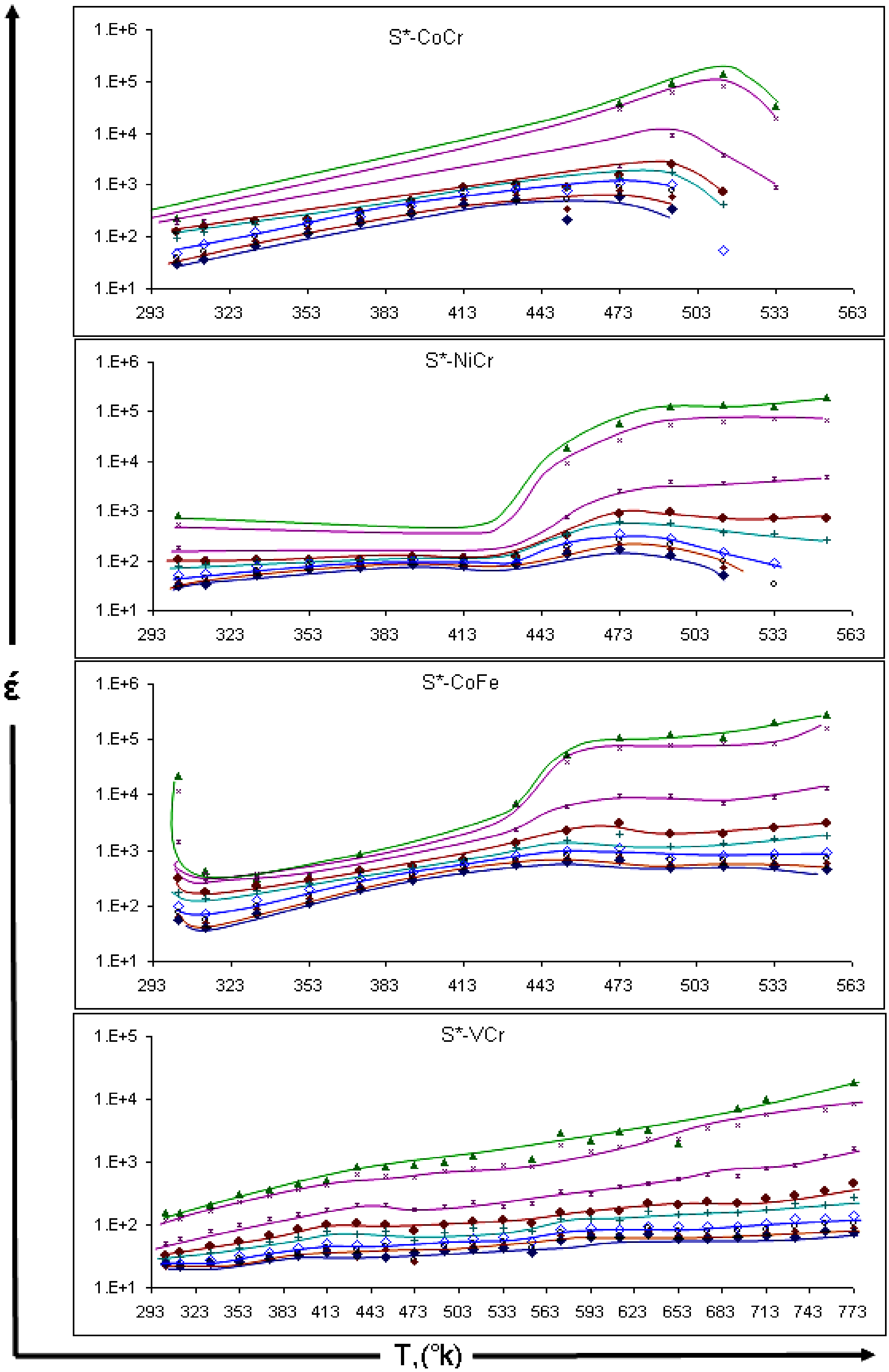

Fig .(13-b) Effect of frequency and temperature on dielectric constant (ε′) for irradiated samples.Where

▲ 500Hz × 1KHz ⁑ 10KHz ◆ 50KHz + 100KHz ◇ 300KHz ○ 500KHz ✦ 700KHz ◆ 1MHz

5 – 4 Dielectric loss factor (ε″)

Figs. 14(a-b) correlates the relation between the dielectric loss factor (ε″) with temperature at different fixed frequencies for all the investigated ferrites irradiated and unirradiated. From the figure it is clear that (ε″) for most samples increases with increasing temperature at all frequencies. Some deviation upon this behavior is observed for unirradiated and irradiated samples S-CoCr, S*-CoCr this needs more investigation and studies .The increase in (ε″) with temperature in these samples is due to the relaxation of the dipole molecules in cooperation with the resulting drop in the relaxation time. This in turn exerts a double effect on the dielectric loss factor, on one hand the friction between the dipoles will be increased and then the increase in energy dissipation. On the other hand the energy required to overcome the internal mechanical friction of the medium will be decreased when the dipole rotates through a unit angle. It is also noticed that (ε″) decrease with the increase of frequency. This decrease can be explained by the fact that the electron exchange between M^{n+} and M^{n+1} ions cannot follow the frequency of the applied field. The decrease in (ε″) with frequency agrees well with Deby's type relaxation-process [11].

All samples exhibit dispersion due to Maxwell interfacial polarization [32], in agreement with phenomenological theory [33]. This behavior of dielectric may be explained qualitatively by supposing that the mechanism of the polarization process in ferrite is similar to that of the conduction process. Iwauchi [6] has pointed out that there is a strong correlation between the conduction mechanism and the dielectric behavior of ferrites. According to Heikes and Johnson [3] the electronic exchange in our samples may be considered as

$$M^{2+}+Mn^{4+} \leftrightarrow M^{3+}+Mn^{3+}. \qquad (22)$$

M may be Co or Fe ions .

One obtains local displacements of electron in the direction of the applied field. These displacements determine the polarization of the ferrite. It is known that the effect of polarization is to reduce the field inside the medium. Therefore, the dielectric constant of a substance may decrease substantially as the frequency is increased. Also, such a decrease can be attributed to the fact that the electric exchange between Co^{2+} and Fe^{3+} ions cannot follow the external applied field beyond a certain frequency.

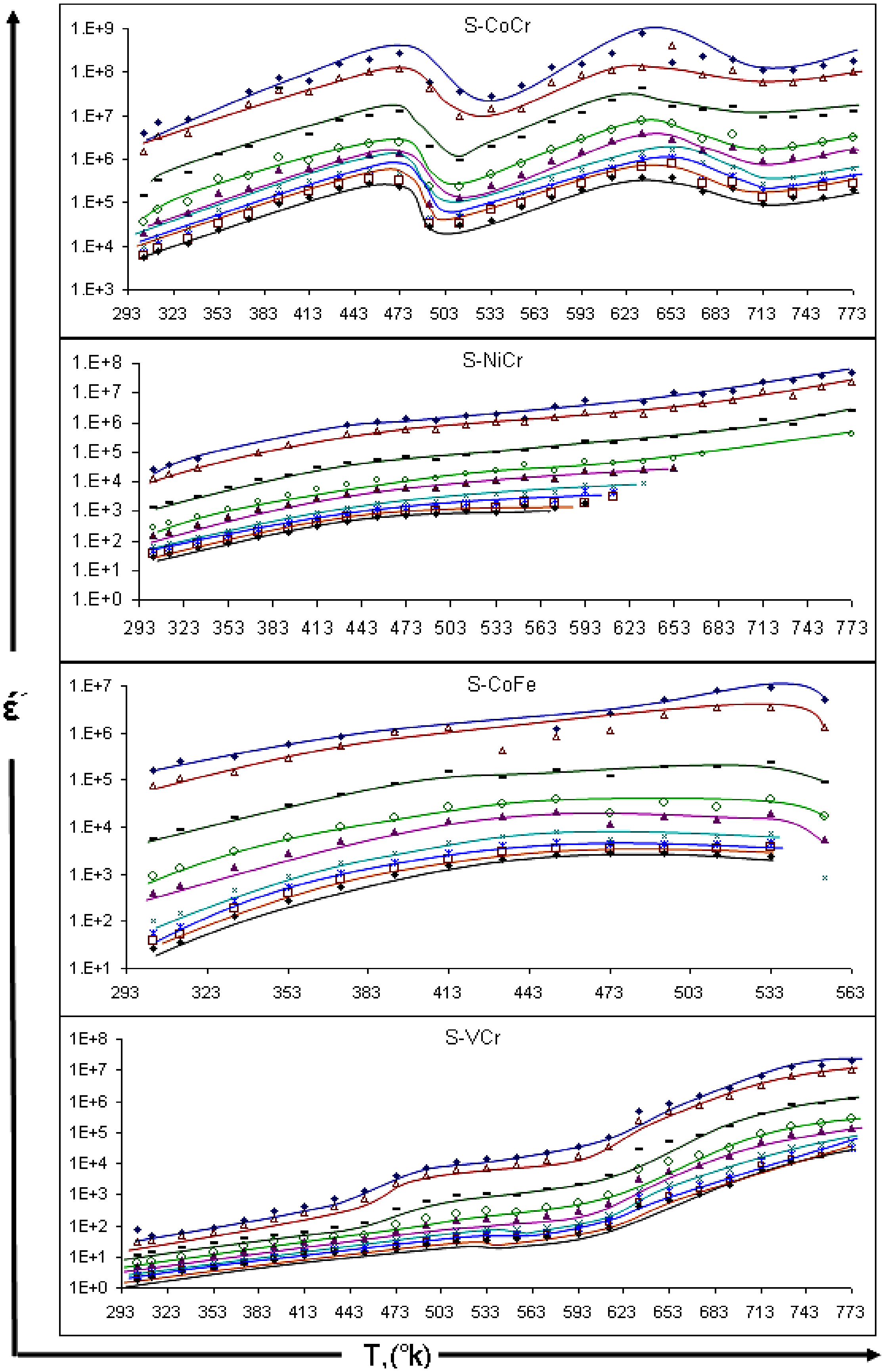

Fig .(14-a) Effect of frequency and temperature on dielectric loss(ε'') for unirradiated samples.Where

| ◆ 500Hz △ 1KHz ▬ 10KHz ○ 50KHz ● 100KHz × 300KHz ✱ 500KHz □ 700KHz ◆ 1MHz |

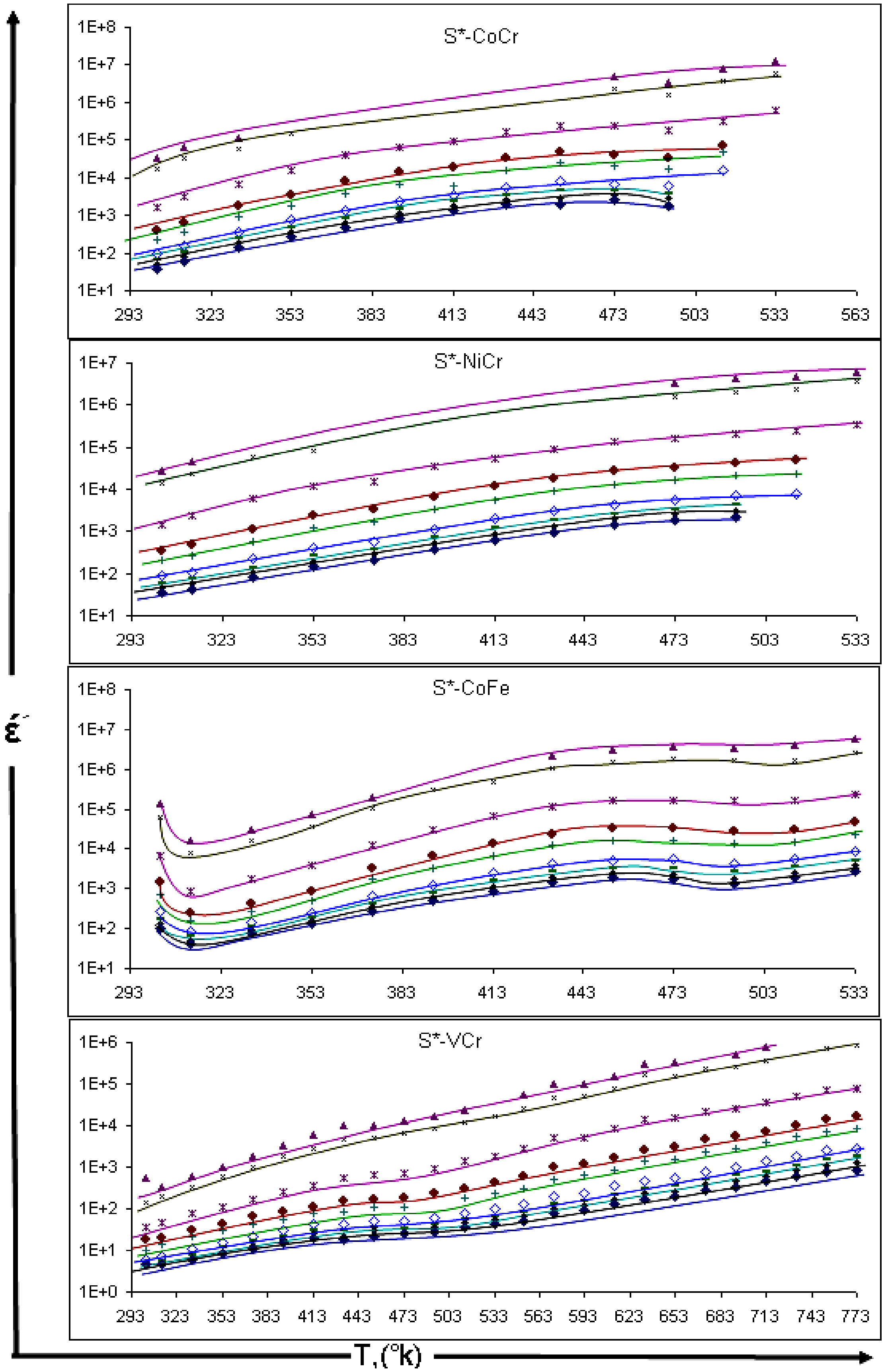

Fig .(14-b) Effect of frequency and temperature on dielectric loss (ε″) for irradiated samples.Where

▲ 500Hz × 1KHz ✱ 10KHz ◆ 50KHz + 100KHz ◇ 300KHz - 500KHz ✦ 700KHz ◆ 1MHz

5 - 5 Composition dependence of σ, ε' and ε''

Dependence of σ, ε' and ε'' on composition of the sample at room temperature and 10^3 Hz is given in Table (8) . It can be seen that σ, ε' and ε'' increase according to the following order:

S-CoCr > S-CoFe > S-NiCr > S-VCr

Table (8) Effect of σ, ε' and ε'' on composition of the sample at room temperature and 10^3 Hz

Composition	At 303(°K)and 10^3 Hz		
	ε'	ε''	σ ($ohm^{-1}. cm^{-1}$)
S-CoCr	5.58E+4	1.48E+6	7.72E-4
S*-CoCr	[2.08E+2]	[1.64E+4]	[1.93E-5]
S-NiCr	1.07E+2	1.27E+4	7.14E-6
S*-NiCr	[5.22E+2]	[1.39E+4]	[7.60E-6]
S-CoFe	6.16E+2	1.58E+4	8.84E-6
S*-CoFe	[1.12E+4]	[6.19E+4]	[3.44E-5]
S-VCr	6.00E+1	3.14E+1	1.75E-8
S*-VCr	[1.16E+2]	[1.43E+2]	[7.94E-8]

*[ ] Irradiated Sample.

The number of vacancies may be established at the B site as Co^{2+}, Cr^{3+}, Ni^{2+}, V^{4+} ions introduce in the samples. Such vacancies initiate the thermal dissociation of oxygen, which in turn increases the number of electrons [17]. Also, a number of M^{2+} ions may be formed during the sample preparation. Such mechanisms will increase the hopping process and consequently increasing **σ** , ε' and ε'' value.